Synthesis and Characterization of Side-Chain Liquid-Crystalline Polyurethane Elastomers

Tzong-Liu Wang,[1] Jung-Shian Tsai,[2] Ching-Guey Tseng[2]

[1]*Department of Chemical and Material Engineering, National University of Kaohsiung, Kaohsiung 811, Taiwan, Republic of China*
[2]*Department of Chemical Engineering, National Kaohsiung University of Applied Sciences, Kaohsiung 807, Taiwan, Republic of China*

ABSTRACT: Side-chain liquid-crystalline (SCLC) polyurethane elastomers with methoxybiphenyl mesogens pendant on the chain extenders were synthesized by the conventional prepolymer technique and condensation reaction. Two SCLC polyurethanes with mesogens having spacers of six and eight methylene units were prepared. The structures of the mesogenic units and SCLC polyurethanes were confirmed by Fourier transform infrared and ^{1}H-NMR. The polymer properties were also studied with solubility tests, water-uptake measurements, and inherent-viscosity measurements. The tensile properties indicated that both SCLC polyurethanes were thermoplastic elastomers. Their phase-transition temperatures were studied with differential scanning calorimetry. Wide-angle X-ray diffraction studies revealed the existence of liquid-crystalline phases for both SCLC polyurethanes. Polarizing optical microscopy investigations further confirmed the thermotropic liquid-crystalline behaviors and smectic mesophases of both samples. Thermogravimetric analysis results showed a more rapid degradation in the initial stage and a slower degradation process in the latter stage for both SCLC polymers in comparison with those of the linear starting polyurethane. © 2005 Wiley Periodicals, Inc. J Appl Polym Sci 96: 336–344, 2005

Key words: differential scanning calorimetry (DSC); elastomers; liquid-crystalline polymers (LCP); polyurethanes; X-ray

INTRODUCTION

Side-chain liquid-crystalline (SCLC) polymers are of both theoretical and practical interest because they combine the anisotropic properties of monomeric liquid crystals with polymeric properties. Their unique behavior is caused by the specific structure, which consists of a polymer chain, a flexible spacer, and a mesogenic unit. Through the variation of the individual structural parts (the polymer backbone, spacer, and mesogenic unit), polymer molar mass, polydispersity, and tacticity, the liquid-crystal behavior can be successfully controlled.[1–4] Therefore, SCLC polymers are of special interest for applications in data storage systems, in piezoelectric, pyroelectric, and ferroelectric devices, and in other systems that require nonlinear optical characteristics.[5–8]

It has also been indicated that if SCLC polymers are elastomers, they can couple the response of liquid crystals and elastomeric networks to applied stress fields.[9,10] The elastomer acts as a matrix through which stress is transferred to the liquid-crystalline side groups, which respond to the applied mechanical field with alignment.

On the other hand, thermoplastic polyurethane (PU) elastomers (i.e., segmented copolyurethanes) are block copolymers of the $(A–B)_n$ type, consisting of alternating soft and hard segments.[11–13] The soft segment is typically a long-chain polyol, which is a polyester diol, polyether diol, or polyalkyl diol with a molecular weight of 500–5000. The hard segment generally consists of an aromatic diisocyanate chain extended with a low-molecular-weight diol or diamine (i.e., chain extender).[14]

The unusual properties of these copolymers are directly related to their two-phase structures. The two-phase feature of the original reaction mixture is due to the thermodynamic incompatibility of the different block polymer segments. It is well-known that the hard segment of thermoplastic polyurethane elastomers (PUTs) can form a thermotropic liquid-crystalline phase when a properly selected diisocyanate and chain extender are used for the polyaddition reaction. The hard segments prepared from 4,4'-dihydroxybiphenyl (DHBP)/hexamethylene diisocyanate,[15] 4,4'-bis(6-hydroxyhexoxy)biphenyl (BHHBP)/4,4'-diphenylmethane diisocyanate (MDI),[16] 4,4'-bis(2-hy-
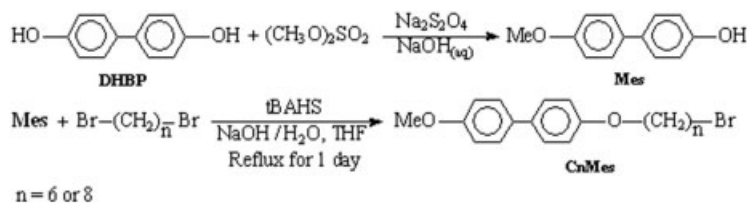
Scheme 1 Synthesis of C$_n$Mes mesogens.

droxyethoxy)biphenyl/toluene diisocyanate (TDI),[17] and BHHBP/TDI[18] pairs are examples of thermotropic liquid-crystalline PUs. However, because linear liquid-crystalline PUs are fluid in the liquid-crystalline state, they do not exhibit cohesive mechanical properties. The coupling of mesogens to a polymer backbone allows the exploration of optical responses to mechanical fields.[19,20]

To our knowledge, SCLC PUs have not been investigated as systematically as side-chain liquid-crystal polymers with acrylic, methacrylic, and siloxane backbones.[21–23] In particular, all these studies were concerned with PUs synthesized from a diisocyanate with a short-chain diol.[22,24–26] This kind of PU had no elastomeric property. As far as we know, the first segmented copolyurethane with SCLC soft segments was synthesized and presented by Hammond et al.[27] The other work was related to the chain extender of a segmented PU carrying a mesogen in the side chain, though with little success.[28]

The aim of our work was to prepare a new series of side-chain liquid-crystalline polyurethane elastomers (C$_n$PUTs). These C$_n$PUTs were designed to exhibit electroresponsive or mechanoresponsive elastomeric properties via functionalization of the chain extender and attachment with a mesogenic unit in the side chain. We have recently presented a new class of SCLC polyurethane elastomers containing 2,2-bis(hydroxymethyl)propionic acid as the chain extender.[29] In this article, we report a subtle synthesis and initial characterization of the other class of C$_n$PUTs with methoxybiphenyl mesogens pendant on the chain extender [1,1,1-tris(hydroxymethyl)propane (TMP)]. Further work will be performed to study their mechano-optic applications.

EXPERIMENTAL

Materials

MDI (DuPont, Inc., Wilmington, DE), methyl isobutyl ketone (MIBK; Hayashi Chemicals, Tokyo, Japan), N,N-dimethylformamide (DMF; Tokyo Chemicals, Tokyo, Japan), and dimethyl sulfoxide (DMSO; Nacalai Tesque, Inc., Kyoto, Japan) were distilled under reduced pressure. TMP (Fluka, Buchs, Switzerland), sodium hydrosulfite (Aldrich, Milwaukee, WI), 1,6-di-

bromohexane (Lancaster, Lancashire, UK), 1,8-dibromooctane (Aldrich), sodium hydride (Showa Chemicals, Tokyo, Japan), triethylamine (Nacalai, Kyoto, Japan), DHBP, tetra-n-butylammonium hydrogensulfate (TCI; Tokyo Chemicals, Tokyo, Japan), dimethyl sulfate, and tetrahydrofuran (THF; Tokyo Chemicals) were used as received. Poly(tetramethylene ether glycol) (PTMG; DuPont, Inc.; M_n = 1000) was degassed in vacuo at 55°C and 600 Pa (4.5 mmHg) for 3 h to remove any absorbed water.

Synthesis of 4-methoxy-4′-hydroxybiphenyl (Mes)

The synthesis of the mesogenic unit (Mes) was referred to the method described in some former literature.[21,30] The reaction is given in Scheme 1.

Synthesis of 1-bromo-n-(4-methoxy-biphenyl-4′-oxy) alkane (C$_n$Mes)

This compound was synthesized according to the literature data[31] and is also shown in Scheme 1. The purity of the obtained product was verified by thin-layer chromatography and NMR analysis. The compound synthesized from Mes and 1,6-dibromohexane was designated C$_6$Mes. The yield was about 80%. C$_8$Mes was prepared in a similar manner, also with a yield of about 80%.

Synthesis of the segmented PUT

PU was synthesized by a two-step technique (Scheme 2). The isocyanate-terminated prepolymer was prepared by the reaction of 20.0 mmol of MDI and 10.0 mmol of PTMG in 70 mL of DMF at 80–85°C for 3 h. This solution was then chain-extended with 10.0 mmol of a TMP (in 15 mL of DMF) solution at the same temperature for another 3 h to obtain the PUT.

Yield: 85%. Fourier transform infrared (FTIR; KBr, cm^{-1}): 3400–3200 ($\nu_{O—H}$), 3300 ($\nu_{N—H}$), 1732 ($\nu_{C=O}$, free), 1712 ($\nu_{C=O}$, hydrogen-bonded), 1110 ($\nu_{C—O}$, C—O—C). ^{1}H-NMR [δ, ppm, deuterated chloroform (CDCl$_3$)]: 1.62 (t, —OCH$_2$C$\underline{H}_2$), 3.41 (m, —OC$\underline{H}_2$CH$_2$), 3.87 (s, Ph—CH_2—Ph), 4.16 [s, C(=O)OCH_2], 4.30 (broad, —CH$_2$O$\underline{H}$), 7.07, 7.26 (m, phenyl), 9.48 [s, NH—C(=O)O].
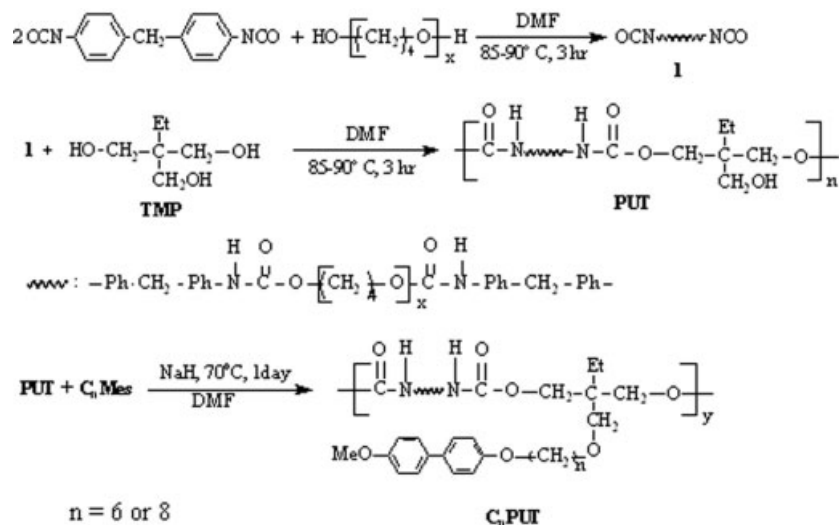
Scheme 2 Synthesis of SCLC segmented PUs.

Synthesis of C$_n$PUT

A solution containing 4.90 g (ca. 3.00 mmol of the —OH group) of PUT in 25 mL of dry DMF was added with 3.00 mmol of C$_6$Mes and then with 3.00 mmol of sodium hydride drop by drop. The reaction was stirred at 70°C for 1 day. The solution was poured into methanol to precipitate the polymer. The product was extracted with chloroform several times to remove C$_6$Mes and was dried in a vacuum oven to obtain the SCLC PU. This polymer was designated C$_6$PUT. Similarly, the SCLC PU prepared from C$_8$Mes was designated C$_8$PUT. The reaction is given in Scheme 2.

C$_6$PUT

Yield: 78%. FTIR (KBr, cm^{-1}): 3300 (ν_{N-H}), 1732 ($\nu_{C=O}$, free), 1712 ($\nu_{C=O}$, hydrogen-bonded), 1274 (ν_{C-O}, Ph—O—C asymmetric), 1244 (ν_{C-O}, Ph—O—C symmetric), 1110 (ν_{C-O}, C—O—C), 824 (δ_{C-H}, p-disubstituted aromatic). ^{1}H-NMR (δ, ppm, CDCl$_3$): 0.90 (t, —CH$_2$C$\underline{H}_3$), 1.25 (q, —C$\underline{H}_2$CH$_3$), 1.62 (t, —OCH$_2$C$\underline{H}_2$), 1.20–1.73 [m, —CH$_2$(C$\underline{H}_2$)$_4$CH$_2$—], 3.41 (m, —OC$\underline{H}_2$CH$_2$), 3.44 (t, —CH$_2$—Br), 3.84 (s, Ph—OC$\underline{H}_3$), 3.87 (s, Ph—C$\underline{H}_2$—Ph), 4.00 [t, Ph—OC$\underline{H}_2$—], 4.16 [s, C(=O)OC$\underline{H}_2$], 7.09, 7.27 (m, phenyl of the main chain), 6.95, 7.46 (m, phenyl of the side chain), 8.51, 9.48 [s, N$\underline{H}$—C(=O)O].

C$_8$PUT

Yield: 77%. FTIR (KBr, cm^{-1}): 3300 (ν_{N-H}), 1732 ($\nu_{C=O}$, free), 1712 ($\nu_{C=O}$, hydrogen-bonded), 1274 (ν_{C-O}, Ph—O—C asymmetric), 1244 (ν_{C-O}, Ph—O—C symmetric), 1110 (ν_{C-O}, C—O—C), 824 (δ_{C-H}, p-disubstituted aromatic). ^{1}H-NMR (δ, ppm, CDCl$_3$): 0.90 (t, —CH$_2$C$\underline{H}_3$), 1.25 (q, —C$\underline{H}_2$CH$_3$) 1.62 (t, —OCH$_2$C$\underline{H}_2$), 1.20–1.73 [m, —CH$_2$(C$\underline{H}_2$)$_6$CH$_2$—], 3.41 (m, —OC$\underline{H}_2$CH$_2$), 3.45 (t, —CH$_2$—Br), 3.82 (s, Ph—OC$\underline{H}_3$), 3.87 (s, Ph—C$\underline{H}_2$—Ph), 4.00 [t, Ph—OC$\underline{H}_2$—], 4.16 [s, C(=O)OC$\underline{H}_2$], 7.09, 7.27 (m, phenyl of the main chain), 6.96, 7.48 (m, phenyl of the side chain), 8.51, 9.48 [s, N$\underline{H}$—C(=O)O].

Characterization

IR spectra of the samples were obtained with a Bio-Rad FTS 165 FTIR spectrometer. The spectra were obtained over a frequency range of 4000–400 cm^{-1} at a resolution of 4 cm^{-1}.

The synthesized compounds and polymers were dissolved in CDCl$_3$ and then characterized with ^{1}H-NMR or ^{13}C-NMR with a Varian Unity Inova-500 FT-NMR spectrometer.

The qualitative solubility was determined with 0.01 g of a sample in 2 mL of a solvent.

The number-average (M_n) and weight-average (M_w) molecular weights and molecular weight distributions (M_w/M_n) were determined by gel permeation chromatography with a Waters liquid chromatograph (Milford, MA) equipped with a 410 RI detector and three μ-Styragel columns with DMF as the carrier solvent.

Inherent viscosity (η_{inh}) measurements were taken at a solution concentration of 0.5 g of polymer/100 mL of solvent at 30°C with a Cannon-Fenske viscosimeter (State College, PA).

The water uptakes of PUs were measured from a weight increase after the immersion of the specimens in deionized water for 48 h at room temperature.

Stress–strain data of urethane copolymers were obtained with a universal testing machine (AGS-500A series, Shimadzu, Tokyo, Japan) with a 10-kg load cell and film grips. The crosshead speed was 50 mm/min.

TABLE I
Solubility[a] of C_nMes and Segmented PUs

Sample	Solvent					
	DMF	DMSO	CHCl₃	MIBK	THF	Acetone
C_nMes	2	2	4	0	2	2
PUT	4	4	1	0	1	0
C_6PUT	4	2	1	0	0	0
C_8PUT	4	2	1	0	1	0

[a] A scale for the different degrees of solubility was assigned as follows: 0 = insoluble; 1 = swelling; 2 = slightly soluble when hot; 3 = soluble when hot, precipitating when cold; 4 = soluble when hot; 5 = soluble when cold.

The measurements were made at room temperature with a dumbbell sample (1.2 cm × 0.4 cm).

Differential scanning calorimetry (DSC) thermograms from 50 to 230°C were obtained during second runs after the thermal history was released with a TA Instruments Modulated DSC 2920 analyzer (New Castle, DE) at a heating rate of 5°C/min under a dry nitrogen purge.

Wide-angle X-ray diffraction (WAXD) diffractograms were obtained on a Rigaku Geiger Flex D-Max III (Tokyo, Japan) with Ni-filtered Cu Kα radiation (40 kV and 15 mA) in 0.05° steps from 2 to 60°; the scanning rate was 4°/min.

The optical textures of the mesophases were studied with a Zeiss polarizing optical microscope (Oberkochen, Germany) (magnification = 10 × 20) fitted with a Linkam THMSE 600 heating stage (Surrey UK) at a heating or cooling rate of 5°C/min. Thin films of the polymers obtained by melting between slides were investigated.

Thermogravimetric analysis (TGA) experiments of the urethane copolymers were carried out on films placed in a platinum sample pan with a TA Instruments SDT-2960 analyzer. Sample films ranging from 4 to 5 mg were cut into small pieces, loaded into the platinum pan, and sealed in the sample chamber. The samples were heated from 50 to 600°C under a nitrogen atmosphere at a rate of 10°C/min.

RESULTS AND DISCUSSION

Design and synthesis

The preparation of Mes and C_nMes was conducted according to the reaction shown in Scheme 1. The starting reagent for synthesizing the mesogen was DHBP because of the presence of a biphenyl unit. Subsequently, to obtain the C_nMes mesogen, dibromoalkane was used for the S_N2 substitution reaction. The spacer length could be controlled by dibromoalkane.

The chemical structures of the products mentioned previously were identified, and the progress of the

reactions was monitored primarily with FTIR spectroscopy. ^{1}H-NMR was used to verify the conclusions drawn from IR analysis for all samples.

The synthetic route of PUT and C_nPUT is outlined in Scheme 2. The SCLC PUs were designed to provide a phase-segregated morphology so that the pendent liquid-crystalline groups in the chain extender could exhibit liquid-crystalline behavior while being anchored by the hard domains. As shown in Scheme 2, the preparation of PUT was conducted in a two-step process derived from the conventional prepolymer technique, and a typical PUT with PTMG as the soft segment and MDI–TMP as the hard segment was synthesized. TMP was used as a chain extender and was considered part of the hard segment. There was a pendent hydroxy group in the chain extender of each repeat unit for further reaction with C_nMes into a liquid-crystalline side chain.

The different behaviors of PUT and C_nPUT in some solvents confirmed the attachment of the mesogenic moiety on the PU backbone as well. The qualitative solubility of C_nMes, PUT, and C_nPUT in various solvents is shown in Table I. Because C_nMes was more soluble in chloroform than C_nPUT, the purification of C_nPUT polymers from the unreacted C_nMes monomers was performed by repeated extraction with chloroform. The purity of the obtained polymer products was verified with FTIR and NMR analysis. On the other hand, because of the presence of more polar hard segments, PUT and C_nPUT were more soluble than the mesogens in aprotic polar solvents such as DMF. However, for an even higher aprotic polar solvent, DMSO, C_nPUT was less soluble than PUT because of the attachment of C_nMes to the hard segments of PUT.

The η_{inh} and water-uptake results of the synthesized PUs are shown in Table II. C_nPUT had lower viscosities than linear PUT in DMF. If the solubility of a polymer in a solvent decreases, the polymer is expected to coil up to maximize the polymer–polymer interactions. Hence, when the C_nPUT polymers attached to less soluble side chains were dissolved in DMF, η_{inh} was lower. On the other hand, a longer spacer length in the side chain increases the hydrodynamic volume of a polymer. Hence, C_8PUT had a higher viscosity than C_6PUT. In comparison with the

TABLE II
Properties of Segmented PUs

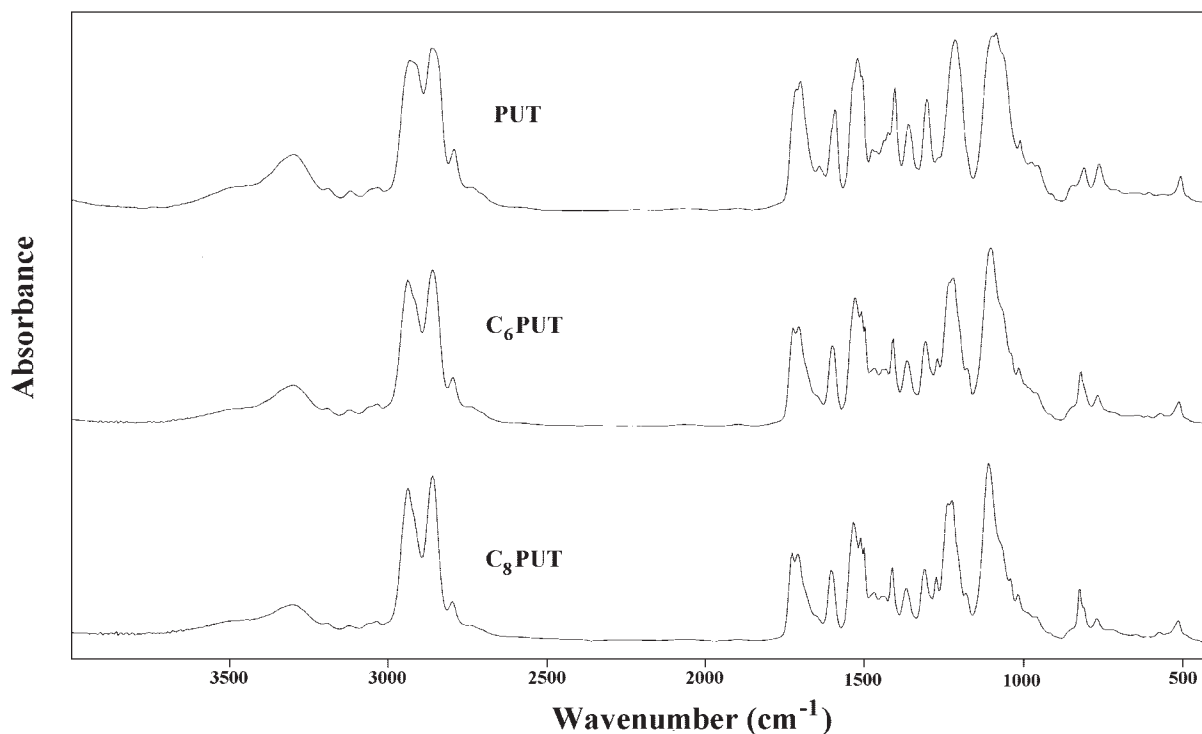| Polymer	$M_n \times 10^{-2}$	PDI	η_{inh} (dL/g)[a]	Water content (%)
PUT	313	1.63	0.68	4.4
C_6PUT	358	1.78	0.42	7.8
C_8PUT	393	1.53	0.46	6.4

[a] At 30°C in DMF.

Figure 1   FTIR spectra of PUT, C$_6$PUT, and C$_8$PUT.

water uptake of typical linear PUT, the higher water uptakes for C$_6$PUT and C$_8$PUT suggested that the attachment of side chains increased the free volume of the polymer. However, a longer side chain due to a longer spacer length increases the entanglement of polymer chains and reduces the free volume between polymer backbones. Consequently, the water uptake for C$_8$PUT was lower than that of C$_6$PUT.

IR and ^{1}H-NMR characterization of PUT and C$_n$PUT

Typical IR spectra of PUT and C$_n$PUT are illustrated in Figure 1. The IR spectra of the SCLC PUs are similar. For both polymers, the absorption bands show the characteristic absorptions of typical PUs. The major NH band at 3300 cm^{-1} is attributable to the N—H band with bonded hydrogen. The carbonyl absorption of the urethane groups is split into two peaks at 1732 and 1712 cm^{-1}, which can be assigned to free and hydrogen-bonded urethane carbonyl groups. The band at 1110 cm^{-1} is assigned to the C—O—C absorption in the soft segment. Furthermore, the peaks at 1274 and 1244 cm^{-1} are ascribed to the asymmetric and symmetric stretching of Ph—O—C, and the peak at 824 cm^{-1} is due to C—H out-of-plane bending in the biphenyl unit. These results indicate that the chemical structure of C$_n$PUT was in accordance with our design.

^{1}H-NMR analysis of PUT and C$_n$PUT confirmed the attachment of the brominated mesogenic group to the starting PU. Because the spectra of the two SCLC PUs are similar, the spectrum of C$_6$PUT is shown as a representative example in Figure 2. In the spectra of PUT and C$_6$PUT, the peaks at about 8.51 and 9.48 ppm are due to the N—H protons of urethane linkages. The aliphatic protons of the PTMG unit existing in —OCH$_2$C$\underline{H}_2$ and —O—CH$_2$ appear at about 1.62 and 3.41 ppm, respectively, whereas —O—CH$_2$ adjacent to the urethane groups can be observed around 4.16 ppm. For PUT, two multiplets corresponding to aromatic protons from MDI units can be observed at 7.07 and 7.26 ppm. When PUT was reacted with C$_6$Mes and transformed into C$_6$PUT, two multiplets at 6.95 and 7.46 ppm appeared and were attributed to resonances of aromatic protons in the biphenyl units. The resonance peaks at about 3.84 and 4.00 ppm, corresponding to aliphatic protons in —Ph—O—CH_3 and —Ph—O—CH_2— were also observed.

Tensile properties

The stress–strain curves for PUT and C$_n$PUT are shown in Figure 3. All the samples showed elastomeric behaviors of typical segmented PUs and were thermoplastic elastomers. In contrast, the higher initial modulus for both SCLC PUs may have been due to a
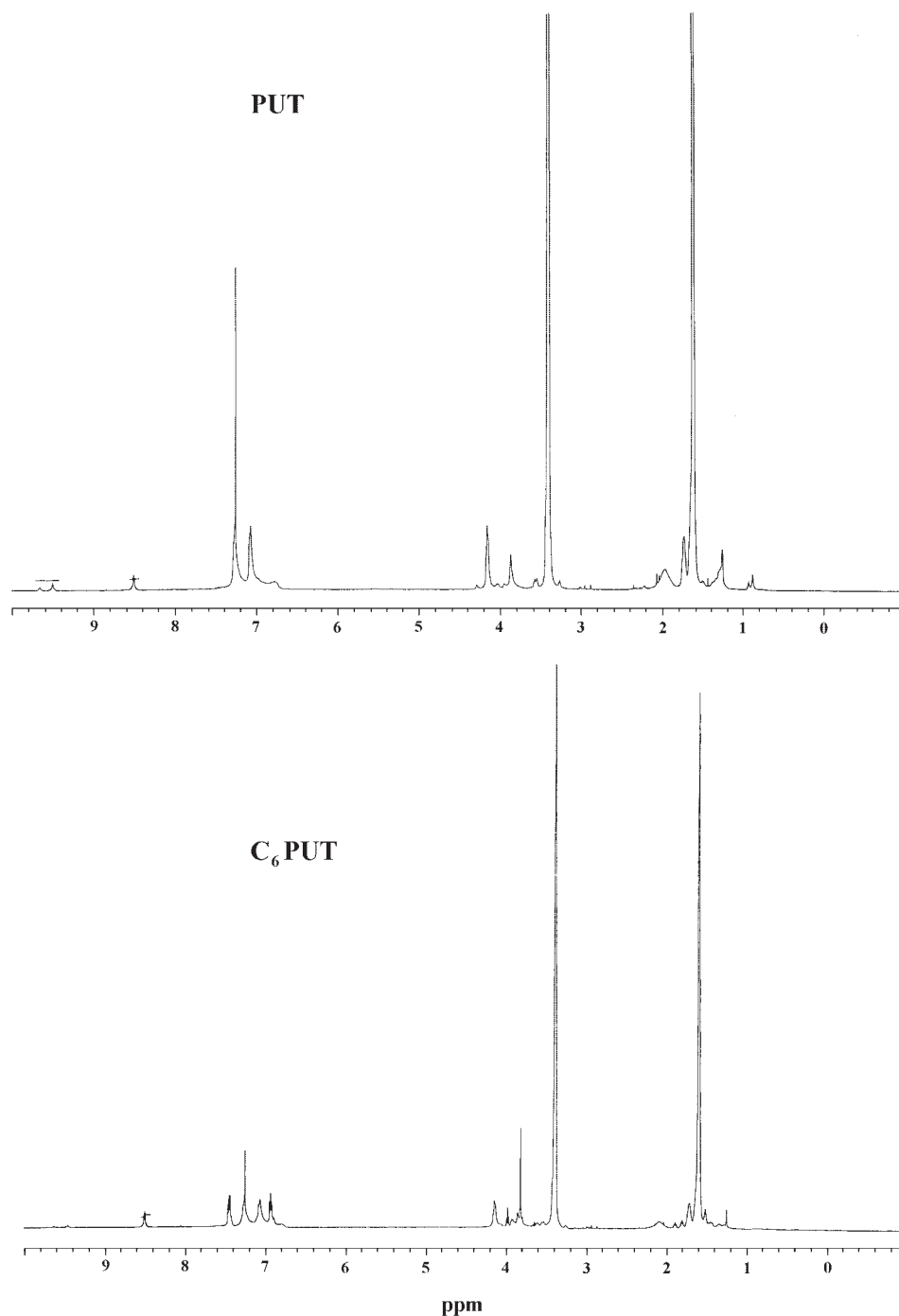
Figure 2 ^{1}H-NMR spectra of PUT and C_6PUT (a representative example of C_nPUT) in $CDCl_3$.

higher weight ratio of hard segments. Hence, both elastomers were more rigid and exhibited smaller extensibility than PUT. On the other hand, the higher tensile strength and extensibility of PUT may be attributed to a higher degree of phase separation in the linear material.

DSC

As shown in Figure 4, the DSC heating curves of both C_nPUTs show a broad peak at about 175–220°C, which

can be ascribed to a complex behavior arising from several transitions. Reasonable transitions may occur in this region, including a continuous melt of the side chains from partial crystallization or an amorphous state and the subsequent formation of a liquid-crystalline phase, a liquid-crystalline phase to an isotropic transition, and a continuous melt of the polymer backbones at higher temperatures. The interchange between the endothermic and exothermic behaviors results in the flat and broad transition peak. Because the
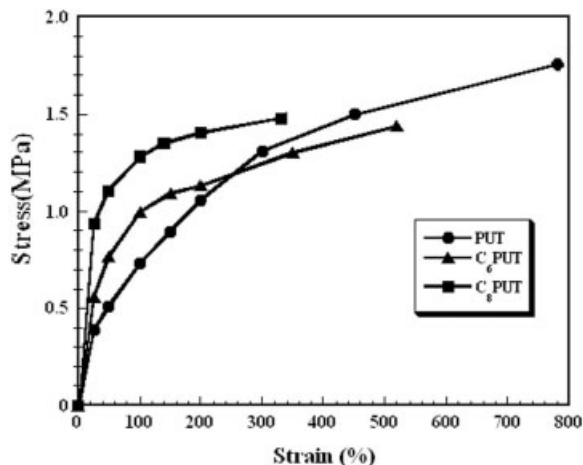
Figure 3 Stress–strain curves for segmented PUs.

Figure 5 WAXD diffractograms of PUT, C_6PUT, and C_8PUT quenched in a dry-ice/2-propanol bath from 180°C.

mesogenic side chains attached to the chain extenders were hard to completely crystallize for a precise melting point, the transition corresponding to the side-chain crystal to the liquid-crystalline phase was not observed.

In the cooling sequences, there is one exothermic peak at 165°C for C_6PUT and 166°C for C_8PUT, which can be ascribed to the isotropic-to-liquid-crystalline phase transition. Similarly, in the lower temperature region, no crystallization peak of the side chains can be observed for the samples. Because the mesogenic groups were attached in the side chain, the reason might be that side chains attached to the chain extenders of the hard segments were not easy to orient to crystallize because of incomplete phase separation (i.e., phase mixing) in the segmented PUs. Hence, the transition was very slow, with an undetectable enthalpy change. As a result, the crystallization was not detected in the heating and cooling sequences. This
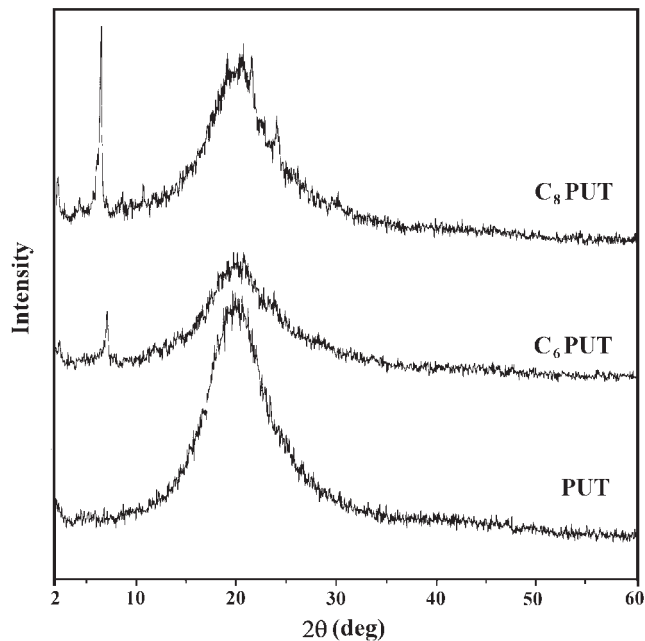
was also confirmed by polarizing optical microscopy (POM) investigations.

Phase behavior in WAXD measurements

WAXD was used to verify the existence of a liquid-crystalline phase. The diffraction patterns were obtained through the heating of these samples to 180°C and their quenching in a dry-ice/2-propanol bath. The diffractograms of C_6PUT and C_8PUT are shown in Figure 5. In comparison with the pattern of PUT, the X-ray diffraction patterns for both samples indicated
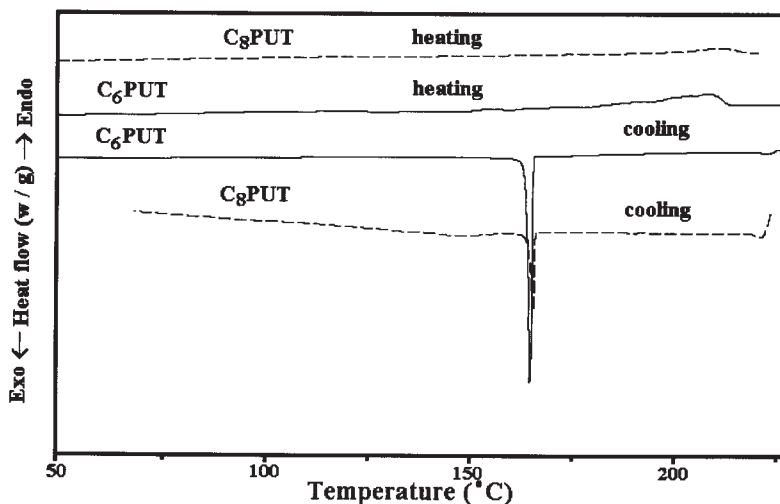

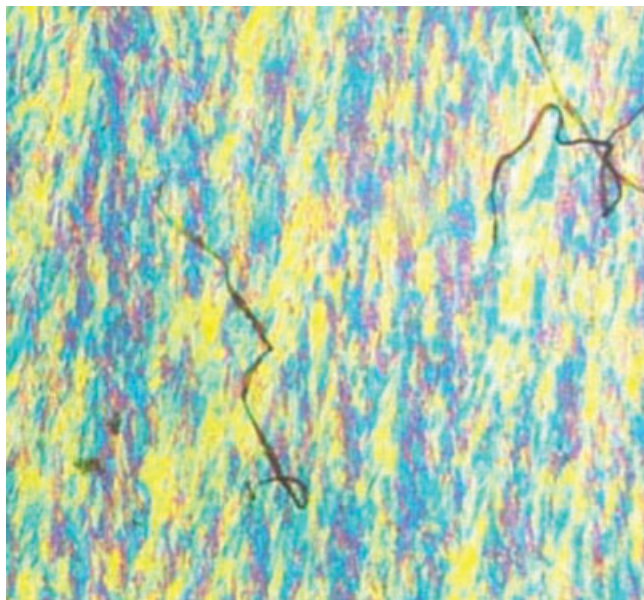**Figure 4** DSC heating and cooling traces of C_6PUT and C_8PUT.

Figure 6 Optical textures of C$_6$PUT between crossed polarizers observed at 165°C upon cooling (original magnification = 10 × 20).
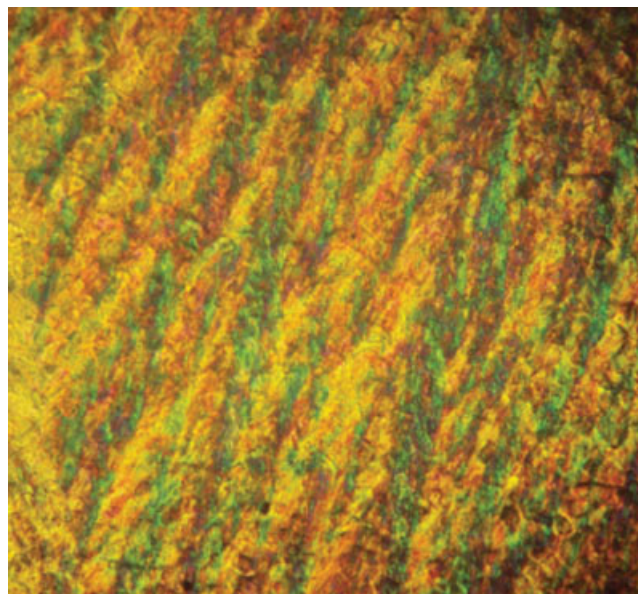

Figure 7 Optical textures of C$_8$PUT between crossed polarizers observed at 166°C upon cooling (magnification = 10 × 20).

that the liquid-crystalline phases were exhibited, as a sharp peak reflection can be observed in the small-angle region. The low-angle peak (2θ = 6.45°) of C$_6$PUT indicates a *d*-spacing of 13.7 Å, whereas the peak (2θ = 7.25°) for C$_8$PUT corresponds to a spacing of 12.2 Å. The two peaks suggest that some very regular interchain spacing of the side chains remained. This may correspond to higher order liquid-crystalline phases, such as smectic or smectic-like soft crystal phases.

Optical texture analysis

The POM investigations of C$_n$PUT revealed well-developed striated, fan-shaped textures in the liquid-crystalline phases, which suggested the formation of mesophases of a smectic type (Figs. 6 and 7) in combination with the WAXD measurements. The textures were obtained upon the cooling of the isotropic phases to 155°C for both samples. The temperature was close to those transition peaks observed in the cooling sequences of the DSC curves.

TGA

The thermal stability for PUT and C$_n$PUT in nitrogen is illustrated in Figure 8 and Table III. The TGA curves for C$_6$PUT and C$_8$PUT show a two-step mechanism for the degradation, which is quite different from the one-step degradation mechanism of PUT. In addition, the temperature at which 10% weight loss occurred ($T_{10\%}$) can be ranked according to the different side-

chain attachments in the following order: PUT > C$_6$PUT > C$_8$PUT. Because it has been indicated that the initial degradation occurs in the hard segments,[32] this may imply that the hard segment attached by a side chain has a different degradation mechanism with that of typical linear PUs. The presence of mesogenic side chains in the hard segment may reduce the thermal stability of segmented PUs.

In comparison with the curves for C$_6$PUT and C$_8$PUT, Figure 8 clearly shows the degradation for PUT was more rapid, and the temperature at which 50% weight loss occurred ($T_{50\%}$) was lower than those of C$_6$PUT and C$_8$PUT. In the second stage, it has been
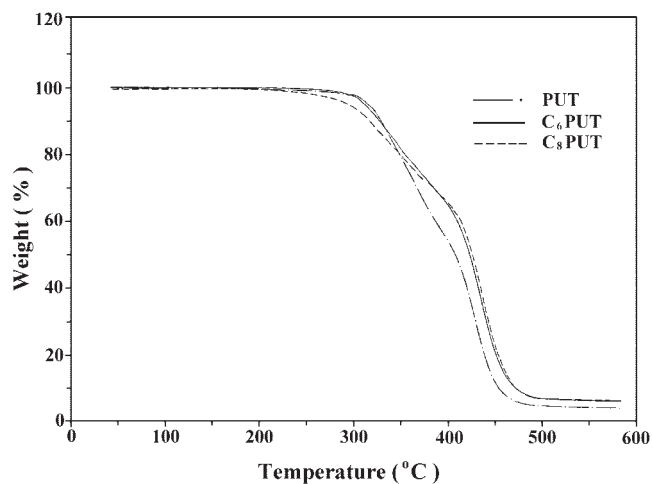

Figure 8 TGA curves of segmented PUs under a nitrogen atmosphere.

TABLE III
Characteristic Temperatures on the TGA Curves

Sample	Degradation in nitrogen	
	$T_{10\%}$ (°C)	$T_{50\%}$ (°C)
PUT	330	407
C_6PUT	328	423
C_8PUT	317	425

indicated that degradation is caused by the soft segments.[33] Hence, the degradation in this stage may be attributed to the fact that the side-chain attachments hindered the degradation of the soft segments. A longer side chain had a larger hindrance effect. Consequently, $T_{50\%}$ increased in the following order, as shown in the figure: PUT < C_6PUT < C_8PUT.

CONCLUSIONS

A new synthetic route was examined to obtain C_nPUTs through the attachment of mesogenic monomers to the chain extender of the PU backbone. The complete synthetic technique and the structural characterization of methoxybiphenyl liquid-crystalline PUs with spacers of six and eight methylene units were presented. The different solubilities of SCLC PUs, with respect to that of the linear starting PU, in some solvents confirmed the attachment of the mesogenic moiety on the PU backbone as well. For both SCLC PUs, different spacer lengths in the side-chain mesogen affected their water uptakes and η_{inh} values. The tensile properties indicated that both SCLC PUs were thermoplastic elastomers and had smaller extensibility than the linear starting PU. DSC curves upon cooling, WAXD studies, and POM investigations indicated that both SCLC PUs exhibited thermotropic liquid-crystalline behavior and a smectic texture. The TGA results for these polymers suggested that the liquid-crystalline segments greatly influenced the thermal stability of the SCLC PUs.

References

1. Craig, A. A.; Imrie, C. T. J Polym Sci Part A: Polym Chem 1996, 34, 421.
2. Percec, V.; Tomazos, D.; Willingham, R. A. Polym Bull 1989, 22, 199.
3. Craig, A. A.; Imrie, C. T. Macromolecules 1995, 28, 3617.
4. Imrie, C. T.; Karasz, F. E.; Attard, G. S. Macromolecules 1993, 26, 3803.
5. Mohlmann, G. R.; Van der Vorst, C. P. J. M. In Side Chain Liquid Crystal Polymers; McArdle, C. B., Ed.; Blackie: Glasgow, 1989; Chapter 12.
6. McArdle, C. B. In Side Chain Liquid Crystal Polymers; McArdle, C. B., Ed.; Blackie: Glasgow, 1989; Chapter 13.
7. Bowry, C.; Bonnett, P. Optical Computing and Processing 1991, 1, 13.
8. Ikeda, T.; Tsutsumi, O. Science 1995, 268, 1873.
9. Davis, F. J. J Mater Chem 1993, 3, 551.
10. Nair, B. R.; Gregoriou, V. G.; Hammond, P. T. Polymer 2000, 41, 2691.
11. Lelah, M. D.; Cooper, S. L. Polyurethanes in Medicine; CRC: Boca Raton, FL, 1986; p 21.
12. Legge, N. R.; Holden, G.; Schroeder, H. E. Thermoplastic Elastomers—A Comprehensive Review; Hanser: New York, 1987; p 13.
13. Walker, B. M.; Rader, C. P. Handbook of Thermoplastic Elastomers, 2nd ed.; Van Nostrand Reinhold: New York, 1988; p 224.
14. Sung, C. S. P.; Schneider, N. S. J Mater Sci 1978, 13, 1689.
15. Tanaka, M.; Nakaya, T. Kobunshi Ronbunshu 1986, 43, 311.
16. Mix, R.; Gahde, J.; Goering, H.; Schulz, G. J Polym Sci Part A: Polym Chem 1996, 34, 33.
17. Penczek, P. K.; Frisch, C.; Szczepaniak, B.; Rudnik, E. J Polym Sci Part A: Polym Chem 1993, 31, 1211.
18. Tang, W.; Farris, R. J.; MacKnight, W. J.; Eisenbach, C. D. Macromolecules 1994, 27, 2814.
19. Finkelmann, H.; Rehage, G. In Liquid Crystal Side Chain Polymer; Finklman, H.; Rehage, G., Eds.; Springer-Verlag: Berlin, 1984; p 99.
20. Davis, F. J. J Mater Chem 1993, 3, 551.
21. Brecl, M.; Zigon, M. Polymer 1999, 40, 6529.
22. Mirceva, A.; Oman, N.; Zigon, M. Polym Bull 1998, 40, 469.
23. Hamara, J.; Liinamaa, K.; Jansson, R.; Sundholm, F. J Macromol Sci Pure Appl Chem 1994, 31, 199.
24. Mirceva, A.; Zigon, M. Polym Bull 1998, 41, 447.
25. Akiyama, E.; Kiode, N. Liq Cryst 1993, 6, 1645.
26. Mihara, T.; Koide, N. Polym J 1997, 29, 138.
27. Nair, B. R.; Osbourne, M. A. R.; Hammond, P. T. Macromolecules 1998, 31, 8749.
28. Jia, X.; Yu, X, Polym Bull 1998, 41, 139.
29. Huang, F. J.; Wang, T. L. J Polym Sci Part A: Polym Chem 2004, 42, 290.
30. Rodriquez-Parada, J. M.; Percec, V. J Polym Sci Part A: Polym Chem 1986, 24, 1363.
31. Akiyama, E.; Koide, N. Liq Cryst 1993, 14, 1645.
32. Ferguson, J.; Petrovic, Z. Eur Polym J 1976, 12, 177.
33. Wang, T. L.; Hsieh, T. H. Polym Degrad Stab 1997, 55, 95.